ACS chemical biology

ARTICLES

pubs.acs.org/acschemicalbiology

Identification and Optimization of Small Molecules That Restore E-Cadherin Expression and Reduce Invasion in Colorectal Carcinoma Cells

Sydney L. Stoops,[†] A. Scott Pearson,[‡,¶] Connie Weaver,[‡] Alex G. Waterson,[†,§] Emily Days,[§] Chris Farmer,[§] Suzanne Brady,[§] C. David Weaver,[†,§] R. Daniel Beauchamp,[‡,∥] and Craig W. Lindsley[†,§,⊥,*]

[†]Department of Pharmacology, [‡]Department of Surgery, [§]Vanderbilt Institute of Chemical Biology, [∥]Department of Cancer Biology, Department of Cell and Developmental Biology, and [⊥]Vanderbilt Program in Drug Discovery, Vanderbilt University Medical Center, Nashville, Tennessee 37215, United States

[¶]Department of Veterans Affairs, Tennessee Valley Healthcare System

Supporting Information

ABSTRACT: E-cadherin is a transmembrane protein that maintains intercellular contacts and cell polarity in epithelial tissue. The down-regulation of E-cadherin contributes to the induction of the epithelial-to-mesenchymal transition (EMT), resulting in an increased potential for cellular invasion of surrounding tissues and entry into the bloodstream. Loss of E-cadherin has been observed in a variety of human tumors as a result of somatic mutations, chromosomal deletions, silencing of the CDH1 gene promoter, and proteolytic cleavage. To date, no compounds directly targeting E-cadherin restoration have been developed. Here, we report the development and use of a novel high-throughput immunofluorescent screen to discover lead compounds that restore E-cadherin expression in the SW620 colon adenocarcinoma cell line. We confirmed restoration of E-cadherin using immunofluorescent microscopy and were able to determine the EC_{50} for selected compounds using an optimized In-Cell Western assay. The profiled compounds were also shown to have a minimal effect on cell proliferation but did decrease cellular invasion. We have also conducted preliminary investigations to elucidate a discrete molecular target to account for the phenotypic behavior of these small molecules and have noted a modest increase in E-cadherin mRNA transcripts, and RNA-Seq analysis demonstrated that potent analogues elicited a 10-fold increase in CDH1 (E-cadherin) gene expression.

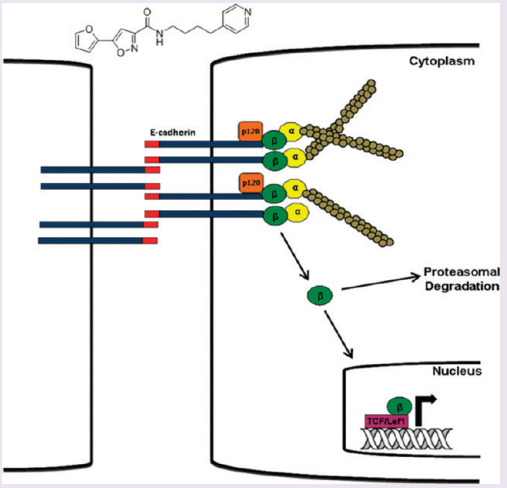

The majority of human cancers arise from epithelial cells, which are held together through junction structures: tight junctions, adherens junctions, and desmosomes.[1] There are several classes of cell adhesion molecules, including cadherins, immunoglobulin-like cell adhesion molecules (Ig-CAMs), the hyluronan receptor CD44, and integrin.[2] The development of malignant tumors, in particular, the transition from benign growths to more invasive or metastatic cancer, is often characterized by a tumor cell's ability to overcome cell-to-cell adhesion and to invade the surrounding tissue, lymph systems, and the circulatory system. During the transition from a normal epithelial cell to a malignant (mesenchymal-like) cell, expression of some of these junction molecules is drastically reduced or switched off. This is often referred to as the epithelial-to-mesenchymal (EMT) transition and is believed to play a prominent role in invasion, extravasion, and colonization during metastasis.[3]

Cell-adhesion molecules are implicated in human carcinogenesis, and recently much attention has been directed toward E-cadherin.[2] E-cadherin is a single-span transmembrane-domain protein that forms homodimers at the cell surface membrane and interacts with the corresponding E-cadherin homodimers of neighboring cells (Figure 1). Aside from cell-to-cell adhesion, E-cadherin is a key component in cell polarity induction and epithelium organization. The loss of E-cadherin function elicits active signals that support tumor-cell migration, invasion, and metastatic dissemination.[4,5]

The loss of E-cadherin function during tumor progression can be caused by genetic or epigenetic mechanisms, the most common of which is down-regulation at the transcriptional level. Repressor transcription factors Snail, Slug, and SIP1, as well as the helix-loop-helix transcription factor E12/E47, have been found to bind to the E2 boxes in the promoter of the E-cadherin gene and actively repress its expression. DNase I hypersensitive site mapping indicated the loss of transcription factor binding, resulting in chromatin rearrangement in the regulatory region of

Received: October 1, 2010
Accepted: January 18, 2011
Published: January 18, 2011

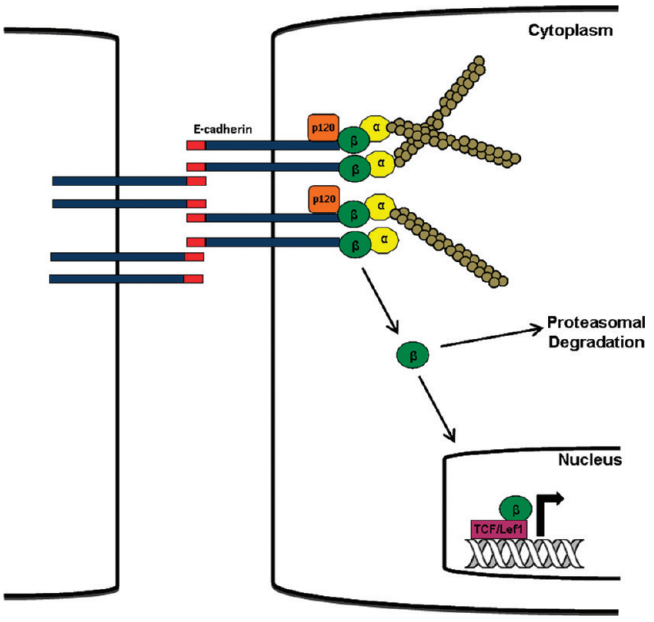

Figure 1. Biological scheme. E-cadherin is a single-transmembrane spanning molecule that forms homodimers at the cellular membrane and interacts in a zipper-like manner with homodimers on neighboring cellular membranes. The cytoplasmic cell-adhesion complex of E-cadherin consists of p120, β-catenin, and α-catenin, which links E-cadherin homodimers to the actin cytoskeleton. These interactions aid in cell polarity induction and epithelium organization. Loss of E-cadherin leads to disassembly of the cytoplasmic cell-adhesion complex and release of p120, β-catenin, and α-catenin into the cytoplasm. There are two pathways for the β-catenin protein to take once released into the cytoplasm. First, β-catenin can be sequestered by the APC/GSK-3β complex and ultimately tagged for proteosomal degradation *via* ubiquitination. Second, upon activation of the Wnt signaling pathway or mutation in the APC/GSK3β complex, β-catenin can no longer be phosphorylated and tagged for degradation and therefore is translocated to the nucleus, where together with TCF/Lef1 transcription factor it modulates the expression of target genes. These genes are known to be involved in cell proliferation and tumor progression.

the E-cadherin gene. As a direct consequence of transcriptional inactivation, the E-cadherin locus is epigenetically silenced by hypermethylation and deacetylation.[6−10] It was shown through cloning and sequencing of the E-cadherin gene promoter that CpG methylation around the promoter region of the E-cadherin gene was present in cell lines that lacked E-cadherin expression and that E-cadherin could be restored in these cell lines upon treatment with the DNA methyltransferase inhibitor 5-azacytidine.[11,12] Deacetylation of histone lysine residues by histone deacetylase (HDAC) enzymes results in chromatin compaction and inactivation of genes. Deacetylation has been shown to occur around the E-cadherin gene promoter region by a repressor complex composed of Snail, HDAC1, and HDAC2. It has been shown that Snail preferentially binds the E2 box in the promoter region, while binding directly to HDAC2 and indirectly to HDAC1. Treatment of cell lines that have reduced E-cadherin expression with Trichostatin A (TSA), a Class I and II histone deacetylase inhibitor, leads to restored expression of E-cadherin in these cell lines.[13,14]

Research has shown that inhibition of E-cadherin expression aids in the EMT in both *in vivo* and *in vitro* models as well as increased metastatic capabilities in *in vivo* models.[15−18] Currently, studies exploring the restoration of E-cadherin expression *in vitro* involve the use of small molecules such as HDAC inhibitors and DNA methyltransferase inhibitors. However, upregulation of E-cadherin expression is merely a side effect of HDAC inhibition or DNA methyltransferase inhibitors by these small molecules but not necessarily the targeted phenotypic response.[14] To further understand the role of E-cadherin in the metastatic process, it would be of value to develop small molecules that restore E-cadherin expression through alternate mechanisms.[19−21]

In this study, we report the development and use of a high-throughput screen to discover lead compounds that restore E-cadherin expression in a metastatic colon adenocarcinoma cell line, SW620, which exhibited low levels of E-cadherin expression. We were able to develop preliminary structure−activity relationships (SARs) around the lead compounds using a Western blot-based E-cadherin restoration assay. In addition, we were able to develop an In-Cell Western assay with the Odyssey Imaging System to quantify EC_{50} values for select compounds. E-cadherin restoration was confirmed *via* visualization of E-cadherin and β-catenin at the membrane after treatment with profiled compounds. The compounds reduce the invasion of colon cancer cells without affecting cellular proliferation. Finally, we show that the compounds increase acetylation of the H4 histone but do not appear to function *via* HDAC inhibition.

RESULTS AND DISCUSSION

High-Throughput Screen To Discover Lead Compounds.

A phenotypic assay suitable for high-throughput screening was developed to identify small molecules that restore E-cadherin expression in SW620 cells. The screen detects E-cadherin restoration at the cell membrane after a 16−18 h incubation with test compound *via* the use of an anti-E-cadherin monoclonal antibody and subsequent secondary antibody-based Alexa Fluor 488 visualization. Images were obtained using a novel plate-based laser-scanning fluorometer, Blueshift Isocyte, that is capable of obtaining images at 2.5−10 μm resolution in all wells of a 384-well plate in 2−10 min/plate. For quantification, a second channel of data was obtained by staining cells with propidium iodide. The propidium iodide counterstain labels cellular nucleic acids, allowing E-cadherin expression levels, as judged by Alexa Fluor 488 fluorescence, to be normalized to cell number on a per-well basis (Figure 2A). The image analysis was performed using BlueImage 2.0, and data was compiled into reports using custom-written applications and Pipeline Pilot. In order to judge assay performance, positive and negative controls were run on each plate. The positive controls consisted of the use of the small molecule HDAC inhibitor trichostatin A and the use of SW620$^{sicld-1}$ cells, which express high levels of E-cadherin by virtue of siRNA knockdown of Claudin-1. After optimization, the screen was found to be suitable for screening in 384-well plates with a Z' averaging >0.5 (Figure 2B). The entire optimized assay protocol was automated on a robotic screening system built around an F3 robotic arm (Thermo Fisher) running on a Polara scheduler (Thermo Fisher).

The automated assay was used to conduct a high-throughput screen of 83,200 small molecules from the Vanderbilt Institute of Chemical Biology library, which was built using a diverse set of molecules available from the ChemDiv and Chembridge collections. The hit threshold was set at 3 standard deviations above the average fluorescent intensity calculated from the test compound wells. The screen revealed 30 confirmed hits, 6 of which produced concentration-dependent effects in the primary screening assay.

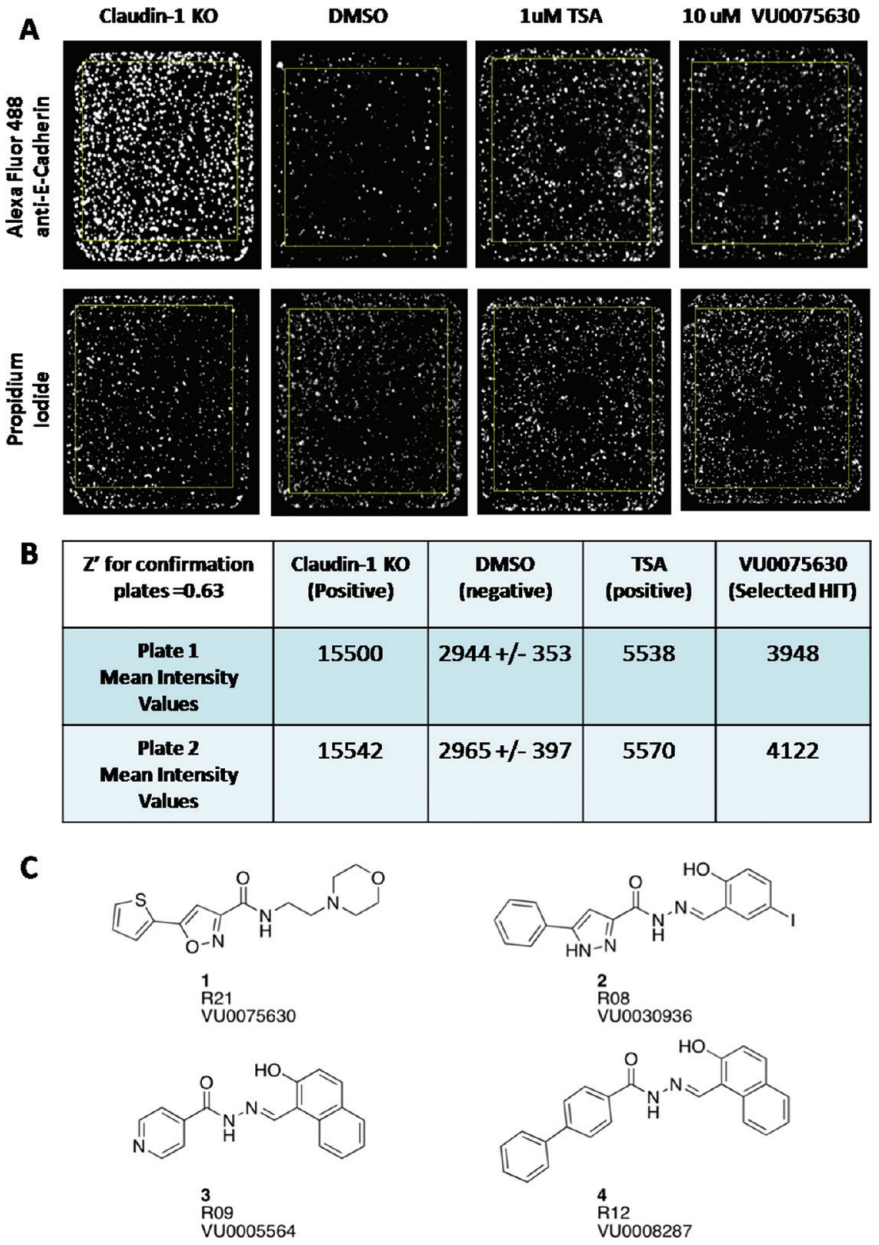

Z′ for confirmation plates =0.63	Claudin-1 KO (Positive)	DMSO (negative)	TSA (positive)	VU0075630 (Selected HIT)
Plate 1 Mean Intensity Values	15500	2944 +/- 353	5538	3948
Plate 2 Mean Intensity Values	15542	2965 +/- 397	5570	4122

Figure 2. High-throughput screen using immunofluorescent staining of human colorectal cancer cells (SW620) identifies increased E-cadherin with treatment of compounds from Vanderbilt Institute of Chemical Biology small molecule library. (A) Dual-color acquisition images show the E-cadherin levels of four representative wells from a 384-well assay plate. (B) The table shows average values for positive (Trichostatin A) and negative (vehicle) controls and a compound selected from the primary screen. (C) Selected hits 1−4 from the E-cadherin restoration screen.

Preliminary SAR. Among the confirmed and validated hits from the initial E-cadherin restoration screen were four compounds with somewhat similar chemotypes (Figure 2C). Each of the hit structures was resynthesized using standard chemistry routes, and the resynthesized molecules were tested to confirm activity in the E-cadherin restoration assay. Because of the instability and poor physiochemical properties of the acyl hydrazone hits R08, R09, and R12 structures (**2**−**4**), we elected to focus our optimization efforts on the R21 structure (**1**). Employing a parallel synthesis library approach, we first explored the eastern amine tail of **1** while maintaining the western 2-thiophenylisoxazole core. This first generation library explored a wide range of functionalized amines as well as structural fragments from **2**, **3**, and **4**.

Selected results from the first libraries are shown in Table 1, wherein compounds were synthesized using standard amide bond forming reactions using commercially available carboxylic acids (**5a**) or acid chlorides (**5b**) and amines. All compounds were evaluated initially at 10 μM in a Western blot assay measuring the ability of the compounds to restore E-cadherin expression in SW620 cells and compared to TSA. The data is expressed as fold change in E-cadherin expression above a DMSO control. Compound **1**, the resynthesized R21 HTS hit, confirmed with a 4.2-fold increase in E-cadherin expression. Elongating the linear linker that serves to attach the morpholine in compound **6a** produced only a slight diminishment of activity (3.5-fold). However, removing the oxygen atom of the morpholine (**6b**) led to a sharp decrease in potency (0.96-fold). Several

Table 1. Synthesis and Evaluation of Initial Compound Libraries[a]

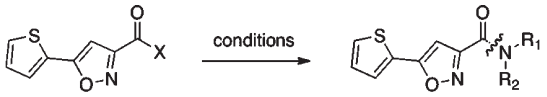

Conditions: For X = OH: HNR_1R_2, EDC, HOBt, DIPEA, THF
For X = Cl: HNR_1R_2, DIPEA, DCM

Cpd	Amine	E-cad	Cpd	Amine	E-cad
1	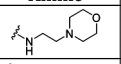	4.25	**6m**	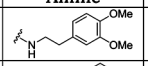	2.71
6a	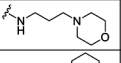	3.51	**6n**	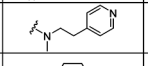	1.63
6b	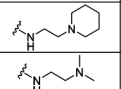	0.96	**6o**	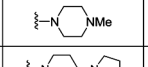	1.25
6c	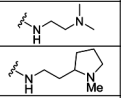	0.97	**6p**	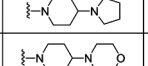	0.84
6d	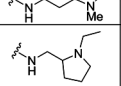	0.86	**6q**	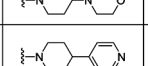	1.06
6e	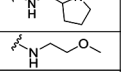	1.13	**6r**	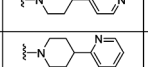	1.18
6f	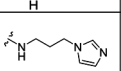	4.29	**6s**	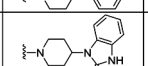	1.13
6g	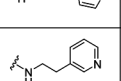	8.11	**6t**	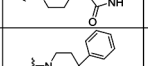	0.92
6h	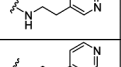	4.97	**6u**	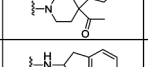	0.90
6i	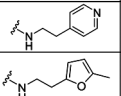	13.25	**6v**	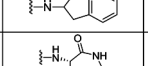	1.36
6j	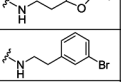	6.98	**6w**	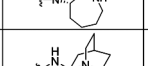	0.75
6k	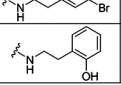	2.29	**6x**	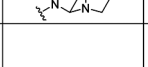	1.19
6l	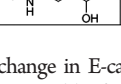	7.30			

[a] Data is fold change in E-cadherin restoration above a DMSO control as measured by Western blot for compound treatment at 10 μM. (TSA = 3.74).

additional attempts to tether a basic amine onto the structure (**6c**−**e**) also met with little success. Interestingly, replacement of the morpholine moiety in **1** with an ether (**6f**) afforded a compound of comparable efficacy (4.3-fold). In addition, a number of heteroaromatic moieties (**6g**−**j**) are well tolerated as morpholine replacements (4.9- to 13.2-fold). In particular, the imidazole **6g** (8.1-fold) and the pyridine **6i** (13.2-fold) produced compounds more efficacious than **1**. Interestingly, substitution on the amide nitrogen is not tolerated, as **6n**, the *N*-Me analogue of **6i** (13.2-fold), provides only a 1.6-fold increase in E-cadherin expression. Additional analogues with a substitution on or adjacent to the amide nitrogen (**6o**−**x**) also displayed sharply reduced potency. Overall, these preliminary libraries provided robust SAR and suggest that the presence of a hydrogen bond acceptor may be a key structural feature leading to enhanced E-cadherin expression.

Optimization of Hit Compounds. With SAR in hand regarding the eastern amide moiety, we next decided to employ a matrix library and explore the western heterobiaryl fragment of **1**, using the eastern amines identified in the first generation library effort (Table 2). We also pursued expansions of the SAR around the amine tail groups of particular interest, especially the pyridine tails of **6h** and **6i**. Selected compounds from Table 1 are included for comparison. As with the morpholine, chain length extension proved successful with an ether-based tail (compare **6f** and **7d**). The 2-pyridyl congener **7g** (12.9-fold) was more than 2-fold more potent compared with **6h** (4.9-fold), being essentially the equal of the 4-pyridyl isomer **6i** (13.2-fold). While a shortened tether was not successful (not shown), the longer butyl chain of **7j** afforded good activity (8.9-fold). Interestingly, we found that phenyl rings with *ortho* substituents, *e.g.*, 2-chlorophenyl derivative (**7l**) and 2-hydroxylphenyl (**6l**), maintained efficacy. In terms of western heterobiaryl SAR, we found that unsubstituted isoxazoles were devoid of activity (data not shown), but a furyl moiety (**8a**−**m**) was a reasonable alternative for the thiophene ring. A methyl thiazole proved to be inferior to the thiophene in nearly all cases (**9a**−**9m**). A phenyl ring was found to be an essentially equipotent replacement for the thiophene (**10a**−**10m**); however, differences were noted depending on the nature of the amine in the eastern tail. Interestingly, neither a pyridine (**11a**), an *o*-flouro (**12a**), nor a *p*-chloro (**13a**) substitution were well tolerated with the morpholine based amine, demonstrating a 2-fold reduction in activity relative to the phenyl substitutent. However, with other eastern moieties, including the ether (**12d**), imidazole (**12e**), furyl (**12f**), and pyrimidinyl (**12h**) containing amines, the *o*-flouro derivative retains potency. Finally, mixed success was obtained with the introduction of heteroaryl substituents, inspired by the acyl hydrazone hits **2**−**4**, into the western portion. A 4-pyridyl analogue was uniformly inactive (not shown), whereas the phenyl pyrazole from **2** (**14a**−**14m**) retained activity in several examples, the best of which (**14j** and **14l**) possessed potency as much as 2-fold better than that of the initial hit **1**. The overall SAR for this matrix library was intriguing, as increased expression of E-cadherin was dependent on the nature of both the eastern and western fragments.

Visualization of E-cadherin Restoration by Selected Analogues. As mentioned previously, all compounds were screened by Western blotting to measure their ability to restore E-cadherin expression in SW620 cells. Compounds that restored E-cadherin to a similar or greater level than compound **1** were further screened in the same E-cadherin assay format in the H520 cell line (Figure 3). Four compounds, **8g**, **8j**, **14j**, and **10k**, were chosen for further profiling on the basis of their performance in the E-cadherin restoration assays and their structural variability. The four compounds selected for profiling in this paper have increased E-cadherin expression in both cell lines and provide examples of successful structural alterations. Additionally, compound **13a** is utilized as a negative control since it does not restore E-cadherin expression in either the SW620 or H520 cell lines. Figure 3 shows the ability of these compounds to restore E-cadherin in both the SW620 and H520 cell lines at a 10 μM dose. It can be seen that the compounds display improved E-cadherin restoration compared to **1** and show slight variability between the two cell lines.

Ultimately, we wanted to develop a method that would allow for an easy determination of concentration response curves. For this, we developed and utilized an In-Cell Western (ICW) assay using the Odyssey Imaging System, which would allow for quadruplicate replicates for each concentration and direct quantification of the intensity of fluorescent secondary antibody in each well (Figure 4A). Use of the ICW assay also allows for fixation, staining, and analysis of the treatments in a single day, approximately 3 h, as opposed to an overnight incubation with

Table 2. Optimization Matrix Based on the R21 Series[a]

Substituent	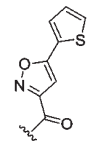	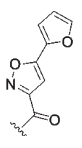	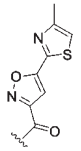	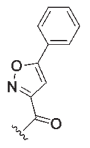	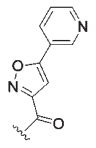	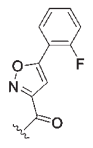	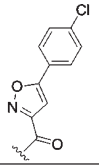	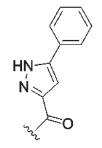
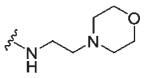	**1** 4.25 (1.91)	**8a** 1.13 (1.25)	**9a** 1.14 (1.01)	**10a** 5.38 (2.80)	**11a** 1.09 (1.06)	**12a** 1.88 (1.08)	**13a** 1.71 (0.94)	**14a** 1.44 (0.95)
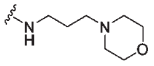	**6a** 3.51 (2.71)	**8b** 1.18 (1.61)	**9b** 0.96 (0.96)	**10b** 2.43 (1.29)	N/A	N/A	**13b** 1.00 (1.28)	**14b** 0.96 (0.73)
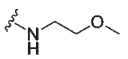	**6f** 4.29 (3.88)	**8c** 2.43 (1.58)	**9c** 1.01 (1.23)	**10c** 3.71 (2.59)	**11c** 1.08 (0.94)	**12c** 2.92 (2.15)	**13c** 1.94 (1.32)	**14c** 1.29 (0.87)
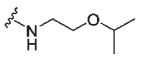	**7d** 5.34 (4.43)	**8d** 3.55 (3.90)	**9d** 1.0 (0.90)	**10d** 4.98 (3.37)	**11d** 1.17 (1.01)	**12d** 3.78 (1.91)	**13d** 2.09 (1.01)	**14d** 2.10 (1.28)
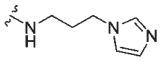	**6g** 8.11 (4.15)	**8e** 2.72 (3.92)	**9e** 1.20 (1.13)	**10e** 4.66 (5.20)	**11e** 1.52 (1.34)	**12e** 3.54 (3.01)	**13e** 1.97 (1.08)	**14e** 1.27 (1.04)
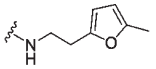	**6j** 6.98 (4.71)	**8f** 3.17 (5.89)	**9f** 1.06 (0.99)	**10f** 4.99 (2.26)	**11f** 1.5 (0.80)	**12f** 4.2 (1.50)	**13f** 1.07 (1.14)	**14f** 2.78 (2.09)
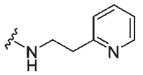	**7g** 12.9 (4.49)	**8g** 6.53 (3.64)	N/A	**10g** 11.99 (3.51)	N/A	N/A	N/A	**14g** 1.72 (1.07)
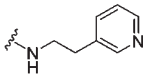	**6h** 4.97 (5.41)	**8h** 4.50 (6.46)	**9h** 1.23 (1.52)	**10h** 4.78 (2.36)	**11h** 1.79 (1.14)	**12h** 4.48 (3.78)	**13h** 2.01 (1.45)	**14h** 2.67 (1.61)
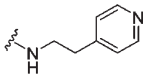	**6i** 13.25 (3.50)	**8i** 8.60 (3.02)	N/A	**10i** 13.69 (1.16)	N/A	N/A	N/A	**14i** 3.50 (1.71)
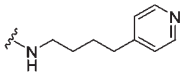	**7j** 8.91 (4.44)	**8j** 9.6 (6.33)	N/A	**10j** 9.60 (4.36)	N/A	N/A	N/A	**14j** 7.66 (5.68)
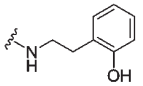	**6l** 7.30 (5.03)	**8k** 4.11 (4.54)	**9k** 0.96 (0.95)	**10k** 11.25 (5.80)	**11k** 1.48 (1.19)	**12k** 1.72 (1.43)	**13k** 1.31 (1.50)	**14k** 6.41 (1.81)
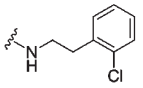	**7l** 8.44 (3.12)	**8l** 7.98 (1.37)	N/A	**10l** 2.52 (0.91)	N/A	N/A	N/A	**14l** 10.27 (1.48)
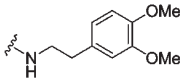	**6m** 2.71 (4.21)	**8m** 2.82 (3.64)	**9m** 0.94 (1.12)	**10m** 2.32 (2.00)	**11m** 1.7 (0.90)	**12m** 2.96 (1.76)	**13m** 0.90 (0.94)	**14m** 4.16 (1.73)

[a] Data is fold change in E-cadherin restoration above a DMSO control as measured by Western blot or In-Cell Western (as seen in parentheses) for compound treatment at 10 μM; N/A = not synthesized (TSA = 3.74 Western blot; 2.37 ICW).

primary antibody necessary with the Western blot. Preliminarily, an optimized single point, 10 μM concentration, ICW assay was developed, and the data for the profiled compounds for both the SW620 and H520 cell lines can be seen in Figure 4A. The ICW assay appeared to trend with the Western blot assay data, confirming that it could be utilized for the development of concentration−response curves (CRC) based on E-cadherin restoration. Representative curves can be seen in Figure 4B for compound **8j** in which the EC_{50} values for E-cadherin restoration in the SW620 cells and H520 cells were 2.13 and 1.25 μM, respectively. The EC_{50} values for **1**, **8g**, **8j**, and **10k** in the SW620 cell line were 10.59, 6.01, 4.47, and 1.49 μM and 5.35, 2.50, 1.61, and 1.99 μM in the H520 cell line, respectively (Figure 5).

While we were able to confirm and quantify that the **1** analogues were restoring E-cadherin, we also wanted to determine the localization of the E-cadherin within the cell. For this, we used immunofluorescent microscopy to visualize the localization of E-cadherin and β-catenin in cells after treatment with the profiled compounds or DMSO (Figure 6). E-cadherin is not present and β-catenin appears dispersed throughout the cytoplasm in the DMSO control and **13a** negative control treated cells. However, the cells treated with compounds known to restore E-cadherin show localization of both E-cadherin and β-catenin to the membrane, especially where cell-to-cell contact is made. Co-localization of these proteins can be seen when the images are merged. This suggests that not only are our compounds capable of restoring E-cadherin protein expression, but E-cadherin is also successfully being transported to the membrane. Additionally, the localization of E-cadherin and β-catenin to the membrane preliminarily suggests that the E-cadherin membrane complex is being formed.

Having shown that the E-cadherin protein is being restored (Figure 3) and that the protein is localizing to the membrane in cells treated with active compounds (Figure 6), we wanted to identify if the restoration was occurring at the transcriptional

dx.doi.org/10.1021/cb100305h |ACS Chem. Biol. 2011, 6, 452–465

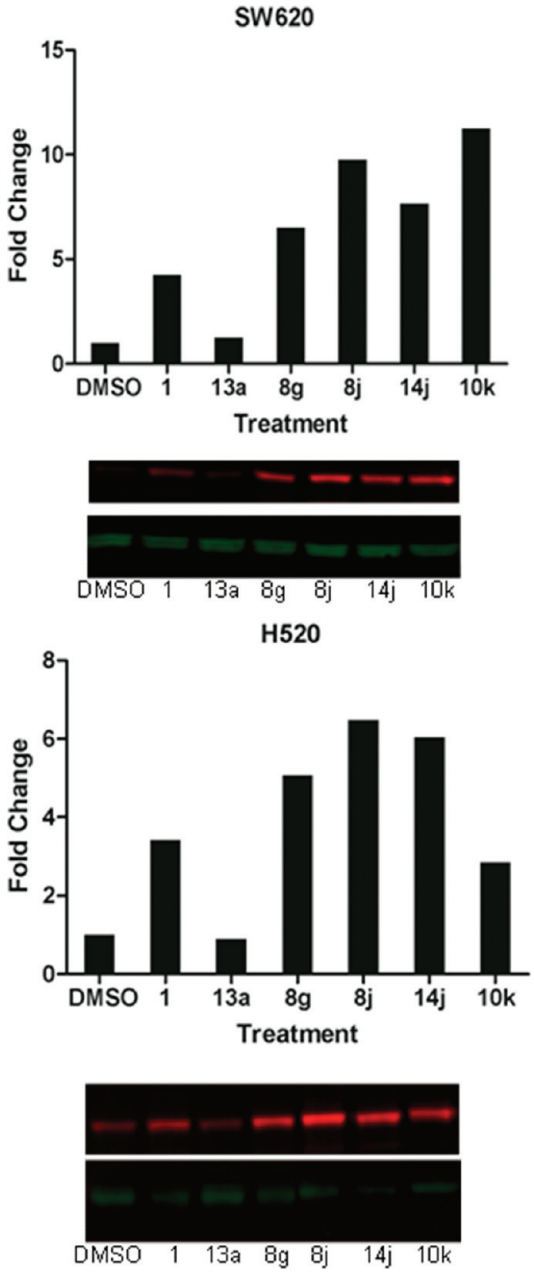

Figure 3. Restoration of E-cadherin by compound treatment. SW620 or H520 cells were treated for 24 h with a 10 μM concentration of compound. Whole cell lysates were collected and subjected to Western blot analysis. Samples were probed for E-cadherin; tubulin was the loading control. Values were quantified as the fold change in E-cadherin expression above the DMSO control.

level. For this we used primers for the E-cadherin mRNA and PCR to determine if there were changes in mRNA levels after treatment of SW620 cells with DMSO, compound **1**, compound **13a**, or compound **8j**. We obserevd that treatment with compounds **1** and **8j** resulted in a modest increase in E-cadherin mRNA transcripts as compared to the DMSO and **13a** treated samples (data not shown). In extension of this finding we decided to send 3 samples to HudsonAlpha Institute for Biotechnology for RNA-Seq anaylsis. RNA-Seq analysis, much like PCR, involves reverse transcription of mRNA samples into cDNA and then sequencing. This provides a very detailed view of both the exact sequence of the genes expressed and the magnitude of the expression. An example can be seen in Figure 6B in which the CDH1 gene reads are shown for each of the three treatments. After analysis cells treated with compound **1** had a 1.4-fold increase in E-cadherin expression and cells treated with compound **8j** had a 10.2-fold increase in E-cadherin expression when compared to the DMSO treated sample. This data further validates that the compounds are restoring E-cadherin protein by enhancing the transcription of CHD1 gene.[22]

The RNA-Seq analysis provided very information-rich data sets for each of the three treatments and comparisons between DMSO and the two compound treated samples. Comparison between the DMSO sample and **8j** sample showed a variety of signaling pathways that are enriched after treatment with compound **8j**. These pathways include EGF receptor signaling pathway (p-value 7.57^{-05}), Notch signaling pathway (p-value 6.56^{-03}), oxidative stress response (p-value 7.18^{-03}), TGF-β signaling pathway (p-value8.15^{-03}), interleukin signaling pathway (p-value 8.57^{-03}), synaptic vesicle trafficking (p-value 8.79^{-03}), integrin signaling pathway (p-value1.08^{-02}), apoptosis signaling pathway (p-value 1.27^{-02}), and inflammation mediated by chemokine and cytokine signaling pathways (p-value 1.29^{-02}). Additionally, there are on-going efforts to further evaluate all of the data presented in the data sets including the synthesis of networking models to understand how genes altered after treatment are interconnected and to aid in the on-going efforts to identify the molecular target.

Cells Remain Viable and Invasion Is Inhibited after Treatment by Selected Analogues. We wanted to determine if the compounds were capable of inhibiting cell proliferation, as uncontrolled proliferation is common in carcinogenesis. For this we utilized a standard bromodeoxyuridine (BrdU) incorporation assay to determine if the compound treatments were inhibiting DNA synthesis. The degree of proliferative effects showed some SAR in the SW620 cells (Figure 7A). **8j** displays significant inhibition of proliferation, while **14j** and **10k** display moderate inhibition in the SW620 cells. However, only **8j** and **10k** showed moderate inhibition in the H520 cells (Figure 7A). While a proliferation effect is advantageous when targeting cancer, the lack of significant inhibition of cell growth further, as seen with **8g** and **14k**, supports the compounds' abilities to decrease invasion by a means other than a cytotoxic effect. This may be important as we are developing compounds that restore E-cadherin and ultimately are targeting reduced invasion and a lower metastatic potential for cancer cells.

Since E-cadherin expression is down-regulated at the invasive front in a variety of cancers, it was important to determine if the analogues of **1** reduced invasion in the SW620 and H520 cell lines.[19−21] The cells were treated with a 10 μM concentration of compound for 24 h and then allowed 72 h to invade through a matrigel-covered chamber. Calcein AM was used to stain the cells on both the top and bottom of the chamber. The fluoroblok membrane within the chamber inserts allows for fluorescence to be read on either side of the chamber without interference. This will account for any inhibition of proliferation, as seen in Figure 7A, as the samples can be normalized to the number of cells remaining in the top chamber. This also confirms that treatment with the compounds is not cytotoxic as Calcein AM is converted to its fluorescent form (Calcein) by living cells. As seen in Figure 7B the compounds were able to reduce the number of invading cells compared to the DMSO control in the SW620 cells as well as the H520 cells (data not shown). Additionally, the negative control, **13a**, did not reduce invasion, as the fold change

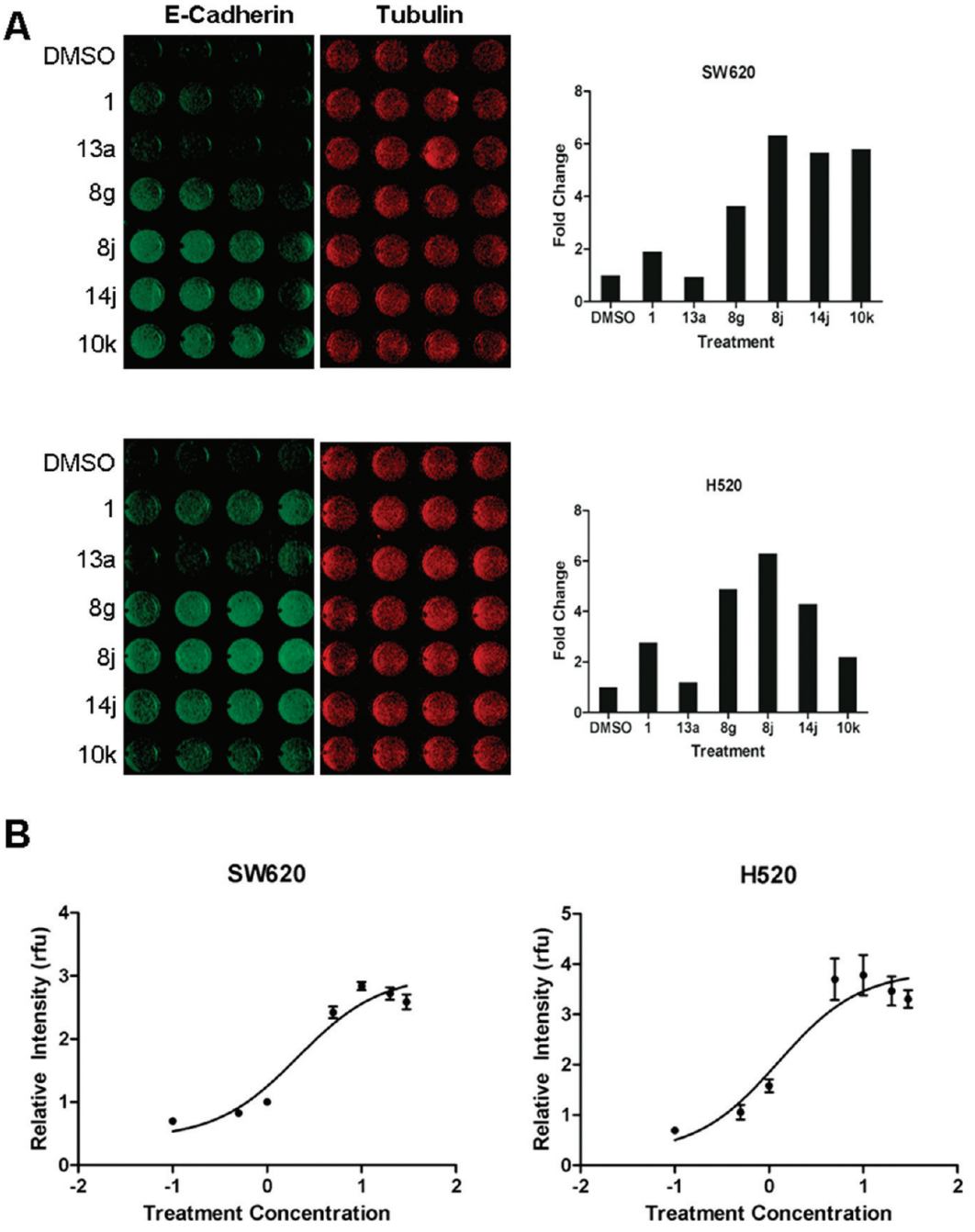

Figure 4. Visualization of E-cadherin and development of concencentration response curves using the In-Cell Western assay. SW620 or H520 cells were treated for 24 h with a 10 μM concentration of compound. (A) After treatment, cells were fixed, permeabilized, and probed for E-cadherin and tubulin (control). The In-Cell Western assay measures fluorescence intensity of the secondary antibodies directly in each well as seen above using the Odyssey Imaging System. For each treatment the intensity values are averaged and normalized to the DMSO control at 1; this is shown as fold change in the corresponding graph. (B) Concentration response curves were developed from seven treatment concentrations from 30 to 0.1 μM (seen as the $\log^{-1}$ in the figure) using the In-Cell Western assay. Each concentration was done in quadruplicate and plotted as the relative intensity of fluorescence.

was similar to that of the DMSO control. This suggests that the decrease in invasion observed with compound treatment alterations is likely to be a result not of toxicity but rather of molecular effects of the compound on the cells.

Efforts To Identify the Molecular Target. Several analogues of **1** were profiled using assays available at MDS Pharma Services against a set of potential targets that might be of importance for epigenetic regulation, such as the sirtuins and matrix metalloproteases (MMP). However, no significant activity was found for the compounds at 10 μM against the sirtuins, nine MMP isoforms, catechol-*O*-methyl transferase, or histamine *N*-methyltransferase. Further, one analogue was evaluated in the MDS Pharma Lead Profiling radioligand binding screen, which consists of a panel of 68 GPCRs, ion channels, and transporter and nuclear hormone receptors. Compound **10e** displayed no significant activity (<50% inhibition at 10 μM), with the lone exception of activity at the imidazoline I_2 central receptor. These data indicate that the ligands discovered in this project are not

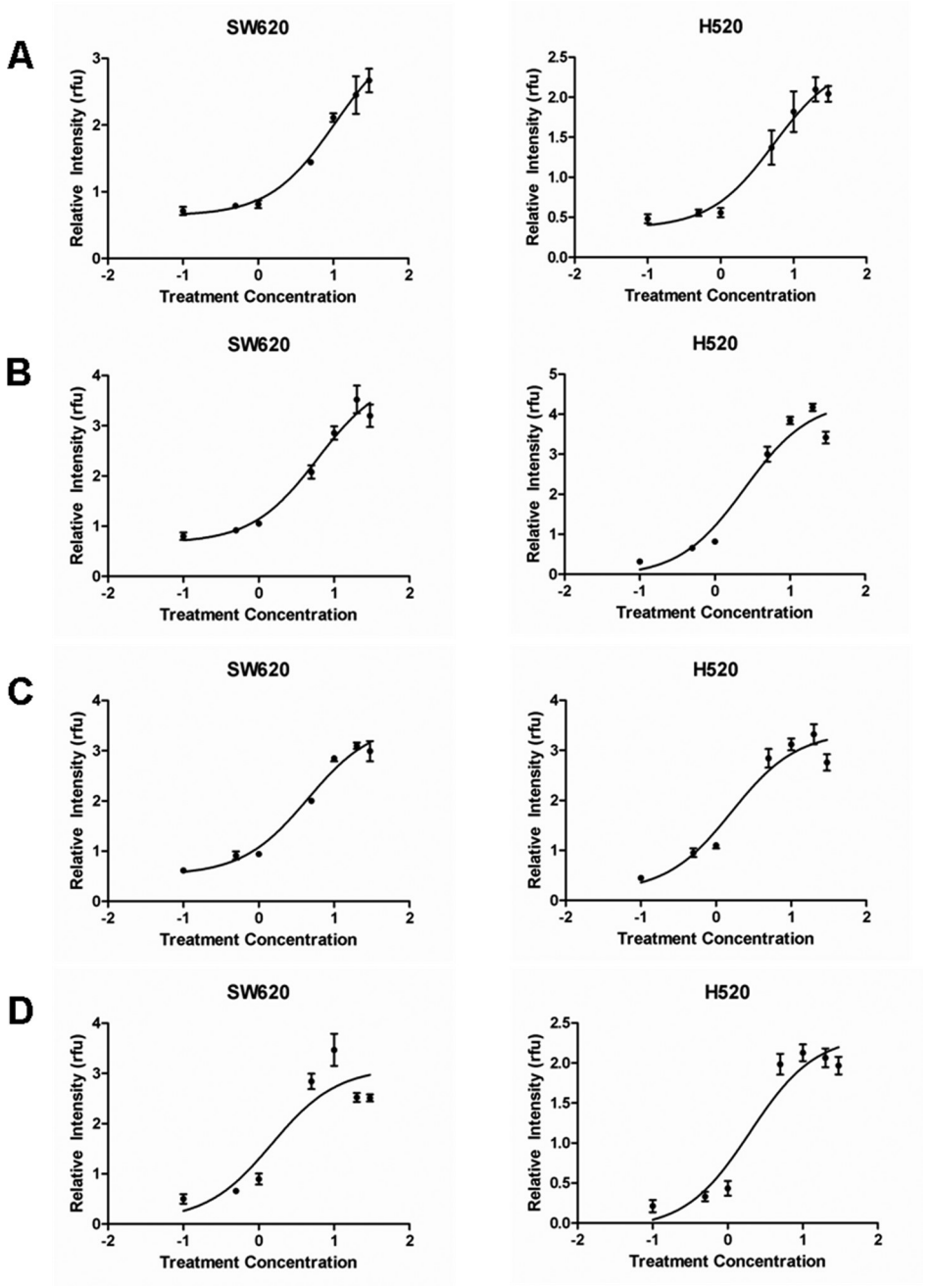

Figure 5. Concentration response curves for profiled compounds. SW620 and H520 cells were treated for 24 h with compound. Concentration response curves were developed from seven treatment concentrations from 30 to 0.1 μM (seen as the $\log^{-1}$ in the figure) using the In-Cell Western assay. Each concentration was tested in quadruplicate and plotted as the relative intensity of fluorescence. (A) Compound **1**, (B) compound **8g**, (C) compound **14j**, and (D) compound **10k**.

broadly promiscuous, which was a concern due to their small size and low molecular weight.

We used our knowledge of TSA, a known HDAC inhibitor and our high-throughput screen positive control, and our results from the MDA Pharma screens to hypothesize that the compounds may be altering histone acetylation and therefore restoring E-cadherin expression. It has been shown that histone deacetylation may lead to transcriptional repression of a gene. More specifically the HDAC1/2-Snail complex has been shown in several cancer models to repress E-cadherin expression directly.[14,16,23] Thus, we treated SW620 and H520 cells with selected compounds and used a Western blot assay to probe for H4 histone acetylation at the Lys9 residue in addition to total H4 histone present in each sample. Figure 8 shows the data expressed as the fold change in histone acetylation above that of a DMSO control. The cells treated with compounds shown to restore E-cadherin have a marked increase in histone acetylation compared to the DMSO control and **13a**. On the basis of published work concerning the involvement of HDACs in E-cadherin repression and cancer and our visualization of increased histone acetylation by treatment with our compounds, we elected to test the compounds for direct inhibition of HDAC isoforms, using commercially available assays measuring

dx.doi.org/10.1021/cb100305h |*ACS Chem. Biol.* 2011, 6, 452–465

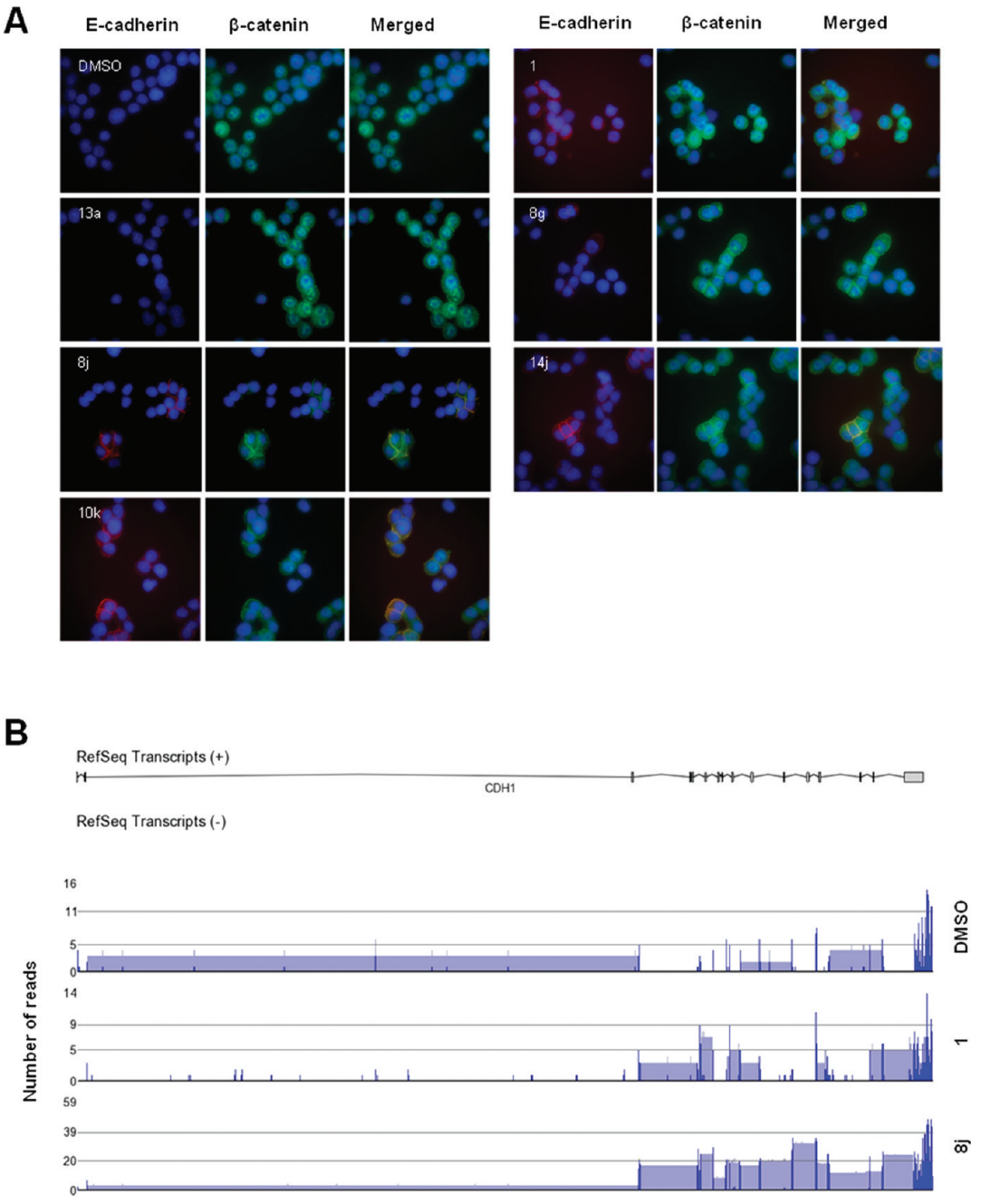

Figure 6. Visualization of E-cadherin and β-catenin after treatment with selected compounds. SW620 cells were treated for 24 h with a 10 μM concentration of compound. (A) Each panel of three images represents a single treatment with immunofluorescent localization of E-cadherin or β-catenin as well as the merged image. Cells were viewed with the 600x total magnification. (B) RNA-Seq experiments and data analysis was conducted at HudsonAlpha Institute for Biotechnology. The panel shows the CHD1 (E-cadherin gene) expression for DMSO, compound **1**, and compound **8j** treated samples. Reads are in bright blue, and the grayish blue boxes between the reads show junctions between exons.

direct inhibition of HDACs 1−11 at Reaction Biology Corporation. A representative member of the series did not show activity against any of the HDACs in the screen. From this we are able to conclude that although our compounds alter histone acetylation, which may explain the restoration of E-cadherin expression, it is not likely to be a result of the direct inhibition of HDAC proteins. However, this does leave a variety of potential molecular targets such as histone acetyltransferase (HAT) and repressor transcription factors, such as SNAIL, which are known to complex with HDACs.

Conclusions. Here we have shown the development and application of two unique assays. The first is a novel high-throughput screen used to identify compounds capable of restoring E-cadherin expression levels in colon adenocarcinoma cells that are deficient in E-cadherin. The second is an ICW assay that permitted the quantification of E-cadherin restoration in a relatively high-throughput manner using the Odyssey Imaging System. The ICW assay allowed for single point screening of synthesized compound libraries, the establishment of concentration

dx.doi.org/10.1021/cb100305h |*ACS Chem. Biol.* 2011, 6, 452–465

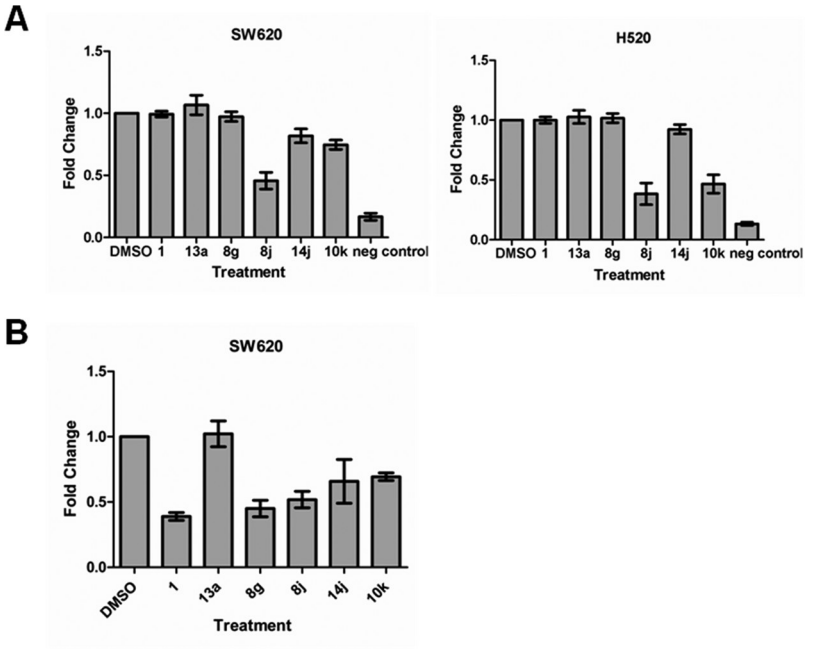

Figure 7. Profiled compounds reduce invasion while having minimal effect on proliferation. (A) SW620 or H520 cells were treated for 48 h with a 10 μM concentration of compound and then analyzed by the BrdU incorporation assay. Each treatment was performed in triplicate, and absorbance was measured at 450 nM. (B) SW620 cells were treated for 24 h with a 10 μM concentration of compound and then plated in the matrigel-covered invasion chamber. Cells were given 72 h to invade and were then strained with Calcein AM and counted on a fluorometer. A fold change of invading cells was calculated as normalized to the DMSO control.

response curves, and identification of an EC_{50}, for each positive compound.

Further, a matrix library approach was undertaken in order to examine a broad spectrum of chemical alterations to both the eastern amine tail and the western heterobiaryl portion of the original hit compound. Such an approach allowed for a relatively rapid synthesis of nearly 100 compounds that were preliminarily screened in both the Western blot and ICW assays. This permitted the visualization of chemical structural trends, allowing for more specific library synthesis in order to further optimize the original lead compound, R21. In total, 200 compounds have been synthesized and screened to date, with the identification of a handful of compounds that restore E-cadherin expression greater than 9- to 10-fold and have EC_{50}'s in the low micromolar range.

Preliminary screening of the more obvious potential targets, such as MMP isoforms, sirtuins, catechol-*O*-methyl transferase, and histamine *N*-methyltransferase, did not uncover the molecular target, while broad screening confirmed that the compounds are not promiscuous and are clean against a range of ion channels and receptors. Further, these compounds were shown to increase histone acetylation in a manner that does not appear to be dependent on HDAC inhibition. We also noted a modest increase in E-cadherin mRNA transcripts, and RNA-Seq analysis demonstrated that potent analogues, such as **8j**, elicited a 10-fold increase in CDH1 (E-cadherin) gene expression.

Thus far, the discrete molecular target remains elusive, and more complex techniques and strategies must be undertaken in order to identify the molecular target of these compounds. However, these compounds may represent a starting point for the development of small molecules that treat metastatic colon cancer by reversing the EMT phenotype. Further work to define the molecular target and further characterization of the mode of action of these compounds is ongoing and will be reported in due course.

METHODS

Cell Culture. A colorectal adenocarcinoma cell line, SW620, and a squamous cell lung carcinoma cell line, H520, were obtained from the American Type Culture Collection (Manassas, VA) and maintained in a humidified atmosphere of 5% CO_2 in air at 37 °C. The cells were routinely cultured in RPMI 1640 supplemented with 10% fetal bovine serum (Atlanta Biologicals, GA) and 100 μg/mL penicillin-streptomycin.

High-Throughput Screen. The metastatic human colon cancer cell line SW620 was selected for this cell-based assay on the basis of their low levels of E-cadherin expression.[24] The high-throughput screening assay was accomplished by modifying the E-cadherin immunoassay from a microscope-based protocol to an automated, HTS-compatible assay in 384-well plates. Variables such as cell concentration and media content, plate type, antibody concentrations, incubation times, and fluorescent indicators were systematically tested to achieve the best overall signal-to-noise ratio and uniformity across the wells of the assay plates. The optimal conditions, which best reproduced previous microscopy data showing trichostatin-A (TSA)-induced increases in E-cadherin staining, were determined as follows: Groups of 10−20 batches of cell plates were seeded on 384 black-walled, clear bottom plates[25] at 4000 cells/20 μL/well in RPMI (Invitrogen), 10% heat-inactivated FBS (Invitrogen), 1% PenStrep (Invitrogen) for 24 h followed by media exchange and 16−18 h pretreatment of TSA control or test compounds (ChemDiv, ChemBridge) in serum-free RPMI (Invitrogen) using a Vprep liquid handler (Velocity 11/Agilent). Compound preparation was conducted by transferring 10 mM DMSO stocks of test compounds with an ECHO 550 (Labcyte) into dry polypropylene plates. Compounds were diluted to 10 μM in RPMI using a MicroFill (BioTek). Overnight compound treatment was performed at 37 °C with 5% CO_2 in a Cytomat II Incubator (Thermo Fisher). The process of fixation and antibody staining was conducted using a Vprep, an ELx405 plate washer (BioTek), and Multidrop (ThermoFisher). The process was integrated and time locked using a F3 robotic arm (Thermo Fisher) run with a Polara (Thermo Fisher) scheduler.

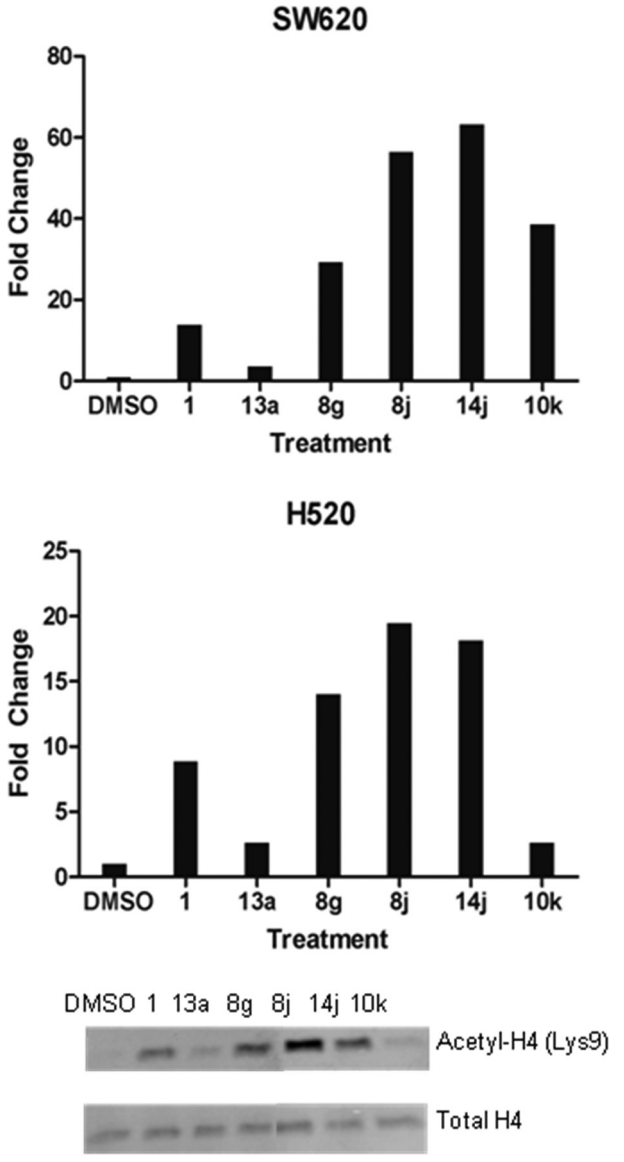

Figure 8. Compounds increase H4 histone acetylation. SW620 or H520 cells were treated for 24 h with a 10 μM concentration of compound. Nuclear fractions were isolated and subjected to Western blot analysis. Samples were probed for Histone H4 acetylation (Lys9) and total Histone H4. Values were quantified as the fold change in histone acetylation above the DMSO control. The blot was also probed with Parp1/2 and RhoGDI to confirm clean fractionation for each sample (not shown).

To decrease the time required during the screening process, steps from the initial microslide staining protocol were consolidated during the HTS validation by combining the permeabilization and blocking steps and the secondary antibody and propidium iodide counterstain steps. Each plate was removed from the Cytomat incubator in a time controlled stagger, and the fixation step was completed on the Vprep by removing compound treatment medium and washing one time with phosphate-buffered saline (PBS) (Invitrogen) followed by RT methanol for 15 min. Next, the cell plate was transferred to the ELx405 washer to remove methanol and washed for two cycles with 50 μL/well PBS. Twenty microliters per well of a mouse monoclonal antihuman E-cadherin antibody (BD Transduction Laboratories) was diluted to a concentration of 625 ng/mL in ice-cold PBS containing 0.2% (v/v) TritonX-100, 1% (w/v) BSA and added to the cell plates using the Multidrop dispenser. The plates were then lidded and incubated 60 min at RT. Cell plates were washed for two cycles on the ELx405 washer with PBS. Following the PBS wash, cell plates received 20 μL/well of Alexa Fluor488-labeled goat antimouse IgG (Invitrogen) diluted 1:4000 in ice-cold PBS containing 0.2% (v/v) TritonX-100, 1% (w/v) BSA, and 0.1 mg/mL propidium iodide (BD Biosciences). The plates were lidded and incubated at RT for 45 min. Finally, the cell plates were washed on the ELx405 with for 2 cycles with PBS.

The cell plates were immediately imaged on an Isocyte (Blueshift Biotechnologies/Molecular Devices) at 10 μm resolution. The excitation wavelength was 488 nm. Alexa Fluor 488 and propidium iodide signals were acquired simultaneously using a 510−545 nm band-pass filter and a 600 nm long-pass filter, respectively. Images we analyzed using BlueImage 2.0 by first using the propidium iodide channel to define the regions occupied by cells and then interrogating the pixel intensity in this region in the Alexa Fluor 488 channel. Background fluorescence was subtracted from the Alexa Fluor 488 channel by subtracting values from local pixels outside the area defined by the propidium iodide channel mask. The data were compiled in two ways either using a custom-built application to compile plate data into a final batch format of 3200−6400 test samples per batch or extracted from Microsoft Excel files into summary records using Pipeline Pilot (Accelrys) protocols. Hits were selected by calculating *Z*-scores based on the 320 test compounds wells on each plate. Wells with Z-scores >3 were called hits. Hits were reordered from ChemBridge and ChemDiv and retested in duplicate. Confirmed hits were resynthesized and tested in triplicate on concentration series of test compounds covering a range of concentrations from 30 μM to1.5 nM. Compounds that produced concentration-dependent effects on E-cad expression were confirmed by mass spectrometry and taken forward to for more extensive testing detailed below.

Control wells were used as quality indicators for assay performance. Controls on each plate included 16 wells treated with vehicle (negative controls), quadruplicate wells of cells treated with a dose range from 0.078 to 5 μM of trichostatin-A, and 16 wells plated with SW620$^{sicla-1}$ cells which express high levels of E-cadherin promoted by stable siRNA knockdown of claudin-1.[26] For wells treated with the trichostatin-A concentration series that hit threshold ($Z > 3$) on average corresponded to 40% of the maximum dose. A "checkerboard" plate in which every other well was treated with either vehicle (negative control) or 1 μM trichostatin-A (positive control) was used as the first plate on each screening day to assess response uniformity and to set parameters of image analysis for the entire batch. The suitability for HTS was assessed daily using the Z' statistic [27] with a $Z' > 0.5$ indicating acceptable data.

Compound Synthesis and Characterization. *Amide Formation from an Acid Chloride.* A mixture containing 0.1 mmol of the acid chloride, 0.11 mmol of the amine, 0.25 mmol of the appropriate base, such as MP-carbonate or diisopropyl ethyl amine, and 2 mL of dichloromethane was stirred or rotated for 12 h or until reaction was judged complete by LC−MS analysis. The reaction mixture was filtered if necessary to remove resins or insoluble impurities and the solvents were removed under reduced pressure. The residue was dissolved in a DMSO/methanol mixture and purified by mass-directed HPLC to generate inhibitors.

Amide Formation from a Carboxylic Acid. To a mixture containing 0.1 mmol of the carboxylic acid, 0.11 mmol of the appropriate amine, and 2 mL of dichloromethane was added a sufficient amount of an amide bond forming reagent. Typical conditions were adding 2 equiv of PS-carbodiimide or 1.2 equiv of EDCI, along with 1.2 equiv of HOBt and 3 equiv of diisopropylethyl amine. The reaction mixtures were allowed to stir or were rotated for 12 h or until reaction was judged complete by LC−MS analysis. The reaction mixture was filtered if necessary to remove resins or insoluble impurities, and the solvents were removed under reduced pressure. The residue was dissolved in a DMSO/methanol mixture and purified by mass-directed HPLC to generate samples for testing.

All NMR spectra were recorded on a Varian Inova 400 (400 MHz) spectrophotometer located in the Small Molecule NMR Facility at Vanderbilt University. ^{1}H chemical shifts are reported in δ values in ppm downfield from TMS as the internal standard. Data are reported as follows: chemical shift, multiplicity, coupling constant (Hz), integration. Splitting patterns describe apparent multiplicities and are designated as s (singlet), d, t (triplet), q (quartet), m (multiplet), br. ^{13}C chemical shifts are reported in δ values in ppm. Low-resolution mass spectra were obtained on an Agilent 1200 LCMS with electrospray ionization. High-resolution mass spectra were recorded on a Waters Qtof- API-US plus Acquity system. Analytical thin-layer chromatography was performed on 250 mM silica gel 60 F254 plates. Analytical HPLC was performed on an Agilent 1200 analytical LCMS with UV detection at 214 and 254 nm along with ELSD detection. Flash column chromatography was performed on silica gel (230−400 mesh, Merck) or using automated silica gel chromatography (Isco, Inc. 100sg Combiflash).

Protein Expression: Western Blot Analysis. SW620 and H520 cells (7.5×10^5/mL) were seeded in 6 cm round plate 24 h prior to treatment. Cells were treated with 10 μM concentration of synthesized compound for 24 h in RPMI 1640 supplemented medium and 100 μg/mL penicillin-streptomycin. Total protein was isolated from cells with the use of RIPA lysis buffer with protease inhibitors. Lysates were sonicated for 10 s, incubated on ice, and centrifuged at 13,000 rpm for 15 min at 4 °C. Protein concentration was measured by absorbance at 595 nm using the Bradford assay reagent (Bio-Rad, Hercules, CA) with bovine albumin standards. Ten micrograms of proteins was loaded per sample on to 10% SDS-polyacrylamide gels that were run at 100 V for approximately 1.5 h. Proteins were electrophoretically transferred to polyvinylidene difluoride (Bio-Rad, Hercules, CA) membranes at 100 V for 2 h. After completion of transfer, the polyvinylidene difluoride membrane was incubated with 10 mL of LI-COR blocking buffer (1:1 dilution in PBS; LI-COR Biosciences, Cambridge, U.K.) for 1 h at RT with gentle agitation. To determine E-cadherin expression level, the membrane was incubated simultaneously with the acetyl-E-cadherin (1:1000; BD Transduction Laboratories, San Jose, CA) and anti-α-tubulin (1:20,000; Abcam, Cambridge, MA) in 10 mL of LI-COR blocking buffer with gentle agitation overnight at 4 °C. The next day, the antiserum was removed, and the membrane was washed 3 times in PBS with 0.1% Tween (PBS-T) before addition of secondary antibody conjugated to a fluorescent entity: IRDye 800-conjugated goat anti-mouse IgG (1:10,000) and IRDye-700-conjugated goat anti-rabbit IgG (1:10,000) in 10 mL of LI-COR blocking buffer with gentle agitation for 1 h at RT. At the end of the incubation period, membranes were washed 3 times with PBS-T. The membrane was visualized and analyzed on the Odyssey IR imaging system (LI-COR Biosciences).

Protein Expression: In-Cell Western Analysis. SW620 and H520 cells (5×10^4/100 μL) were seeded in a 96-well plate prior to treatment. Cells were treated with 10 μM concentration of synthesized compound in quadruplicate for 24 h in RPMI 1640 supplemented medium and 100 μg/mL penicillin-streptomycin. The cells were then fixed with 100% methanol for 20 min at 4 °C. The wells were then washed 2 times with PBS, permeabilized in 2% bovine serum albumin (BSA) and 0.2% TritonX-100 in PBS for 30 min at RT with gentle agitation, and blocked in LI-COR blocking buffer for 30 min at RT with gentle agitation. The cells were then incubated with the following primary antibodies: anti-E-cadherin (1:500) and anti-α-tubulin (1:1000) diluted in blocking buffer (1:1 dilution in PBS) for 2 h at RT with gentle agitation. The cells were washed 4 times in PBS-T for 5 min each and then incubated with the following secondary antibodies conjugated to a fluorescent entity: IRDye 800-conjugated goat anti-rabbit IgG (1:1000) and IRDye-700-conjugated goat anti-mouse IgG (1:2000) in blocking buffer (1:1 dilution in PBS) with gentle agitation for 1 h at RT. The cells were washed 4 times in PBS-T for 5 min each followed by a single wash with PBS. All liquid was removed from the wells and the plates were visualized and analyzed on the Odyssey IR imaging system (LI-COR Biosciences).

The assay was further optimized in the following manner (results seen in Table 2). The cells were washed 2 times with PBS, fixed in 100% methanol at RT for 15 min, and again washed 2 times with PBS. The cells were then incubated with the following primary antibodies: anti-E-cadherin (1:200) and anti-α-tubulin (1:2000) diluted in ice cold 2% bovine serum albumin (BSA) and 0.2% TritonX-100 in PBS for 1 h at RT with gentle agitation. The cells were washed 2 times in PBS and then incubated with the following secondary antibodies conjugated to a fluorescent entity: Licor 800-conjugated goat anti-rabbit IgG (1:2000) and IRDye-700-conjugated goat anti-mouse IgG (1:2000) in ice cold 2% BSA and 0.2% TritonX-100 in PBS with gentle agitation for 45 min at RT. The wells were washed 2 times in PBS, dried, and analyzed as previously mentioned.

Immunofluorescence Analysis and Deconvolution Microscopy. SW620 and H520 cells (7×10^4/well) were seeded on 8-well chamber slides for 24 h prior to treatment. Cells were treated with 10 μM concentration of synthesized compound for 24 h in RPMI 1640 supplemented medium and 100 μg/mL penicillin-streptomycin. The cells were rinsed with PBS and fixed with 100% methanol for 15 min at 4 °C. The cells were rinsed with PBS and blocked and permeabilized with 2% BSA and 0.2% TritonX-100 in PBS. The cells were then incubated with the following primary antibodies: anti-β-catenin and E-cadherin diluted in 1% BSA in PBS blocking solution overnight at 4 °C. After 3 washes with PBS, the cells were incubated with appropriate secondary antibodies conjugated to fluorescein (1:200; Sigma, St. Louis, MO), Texas Red (1:500; Invitrogen, Carlsbad, CA), and DAPI (1:2000, Sigma, St. Louis, MO) for 40 min at RT. The cells were washed 3 times with PBS and then mounted with Vectashield mounting medium (Vector Laboratories, Burlingame, CA). Deconvolution microscopy analyses were performed using the DeltaVision Core (Applied Precision) microscope. All images were taken at using a 600x oil immersion objective and converted to TIFF format and arranged using Photoshop 7.0 (Adobe, Seattle, WA).

RNA-Seq Experiment and Analysis. The RNA-Seq experiments and analysis were carried out at HudsonAlpha Institute for Biotechnology (Huntsville, AL). SW620 cells (1.5×10^6/1 mL) were seeded in 3.5 cm dishes, 9 total. Three plates were treated with a 10 μM concentration of DMSO, compound **1**, or compound **8j** for 24 h in RPMI 1640 supplemented medium and 100 μg/mL penicillin-streptomycin. RNA was extracted from each of the samples and quantified prior to shipment to HudsonAlpha. Upon arrival, the 3 samples per treatment were pooled and prepared for sequencing. Raw data was aligned using Tophat and then analyzed through the Cufflinks pipeline on site.[28]

Proliferation Analysis. SW620 and H520 cells (2.5×10^4/100 μL) were seeded in 96-well microtiter plates prior to treatment. Cells were treated with 10 μM concentration of synthesized compound in triplicate for 48 h in RPMI 1640 supplemented medium and 100 μg/mL penicillin-streptomycin. The CycLex Cellular BrdU ELISA Kit from MBL International (Woburn, MA) was used to measure proliferation. The RPMI media was removed and replaced with 100 μL of 1x BrdU label mix in RPMI media for 2 h at 37 °C in 5% CO_2 in the air. The BrdU label mix was removed, and 200 μL of the Fix/Denature solution was added and incubated for 30 min at RT. The plate was drained, incubated with 50 μL of primary antibody for 1 h at RT, rinsed with wash buffer, and incubated with 50 μL of secondary antibody. The wells were rinsed with wash buffer followed by a single rinse with PBS and drained. Fifty microliters of substrate solution was added and incubated for 6 min followed immediately by 50 μL of Stop solution. The change in proliferation was quantified by measuring the absorbance of the dye solution at 450 nm on a microtiter plate reader.

Invasion Analysis. SW620 cells (2.5×10^5/ mL) were seeded in 6-well plates prior to treatment. Cells were treated with 10 μM concentration of synthesized compound for 24 h in RPMI 1640 supplemented

medium and 100 μg/mL penicillin-streptomycin. Next, 40 μL (2.5 mg/mL) of BD Matrigel Basement Membrane Matrix (BD Biosciences, Bedford, MA) was added to the top of the Fluoroblok invasion chambers (BD Biosciences). Then the cells were trypsinized, and 3×10^5/250 μL cells were added to the top of the chamber in serum-free RPMI medium, and 1 mL of RPMI medium with 10% FBS was added to the bottom of the well. Then the plates were incubated for 72 h at 37 °C in 5% CO_2 in the air. Invading cells were stained with Calcein AM as a fluorescent dye to count invading cells using a fluorometer (Molecular Devices Spectramax M5). All experiments were done in triplicate with a total of three independent replicates.

Histone Acetylation Anaylsis. SW620 and H520 cells (7.5×10^5/mL) were seeded in 6 cm round plates prior to treatment. Cells were treated with 10 μM concentration of synthesized compound for 24 h in RPMI 1640 supplemented medium and 100 μg/mL penicillin-streptomycin. The Nuclear Extract Kit from Active Motif (Carlsbad, CA) was used to collect the nuclear fraction from each sample. Twenty micrograms of proteins was loaded per sample on to 10% SDS-polyacrylamide gels that were run at 100 V for approximately 1.5 h. The Western blot protocol is same as previous described in the Protein Expression: Western Blot Analysis section. To determine Histone H4 acetylation, the membrane was incubated with the acetyl-Histone H4 antibody (1:1000; Millipore, Temecula, CA) in 10 mL of LI-COR blocking buffer overnight at 4 °C. The next day, the antiserum was removed, and the membrane was washed in PBS-T before addition of secondary antibody: IRDye 800-conjugated goat antirabbit IgG (1:10,000) in 10 mL LI-COR blocking buffer for 1 h at RT. The membrane was washed in PBS-T and analyzed on the Odyssey IR imaging system. Membranes were stripped with 10 mL of Li-COR stripping buffer (1:5 dilution in ddH_20) for 30 min at RT with gentle agitation followed by three 10-min washes with PBS. Membranes were reprobed with anti-Histone H4 Pan (1:1000; Upstate, Lake Placid, NY), anti-RhoGDIα (1:1000; Santa Cruz Biotechnologies, Santa Cruz, CA), and anti-PARP 1/2 (1:1000; Santa Cruz Biotechnologies, Santa Cruz, CA) in 10 mL of blocking buffer for 1 h at RT. The antiserum was removed, and the membrane was washed 3 times in PBS-T before addition of secondary antibody: IRDye 700-conjugated goat anti-rabbit IgG (1:10,000) in 10 mL of LI-COR blocking buffer for 1 h at RT. At the end of the incubation period, membranes were washed 3 times with PBS-T and analyzed on the Odyssey IR imaging system.

Statistical Analysis. GraphPad Prism Software (GraphPad Software, San Diego, CA, USA) was used to analyze all data other than the high-throughput screening data, which was analyzed as noted above.

■ ASSOCIATED CONTENT

Supporting Information. This material is available free of charge *via* the Internet at http://pubs.acs.org.

■ AUTHOR INFORMATION

Corresponding Author
*craig.lindsley@vanderbilt.edu

■ ACKNOWLEDGMENT

The work was supported by USPHS grants, CA069457 [29], and the Vanderbilt-Ingram Cancer Center Support Grant (CA068485); the GI Cancer SPORE Grant, (CA095103); and the Vanderbilt Institute of Chemical Biology. We are grateful to Natalia Nalywajko, Kate Lornsen, and Michael Williams from the High-Throughput Screening Laboratory at Vanderbilt University. We would like to thank Shawn Levy and the members of his laboratory at HudsonAlpha Institute for Biotechnology for performing the RNA-Seq experiments and data analysis.

■ REFERENCES

(1) Christofori, G., and Semb, H. (1999) The role of the cell-adhesion molecule E-cadherin as a tumour-suppressor gene. *Trends Biochem. Sci. 24* (2), 73–76.

(2) Cavallaro, U., and Christofori, G. (2004) Cell adhesion and signalling by cadherins and Ig-CAMs in cancer. *Nat. Rev. Cancer 4* (2), 118–132.

(3) Steeg, P. S. (2003) Metastasis suppressors alter the signal transduction of cancer cells. *Nat. Rev. Cancer 3* (1), 55–63.

(4) Miyoshi, J., and Takai, Y. (2008) Structural and functional associations of apical junctions with cytoskeleton. *Biochim. Biophys. Acta 1778* (3), 670–691.

(5) Voulgari, A., and Pintzas, A. (2009) Epithelial-mesenchymal transition in cancer metastasis: mechanisms, markers and strategies to overcome drug resistance in the clinic. *Biochim. Biophys. Acta 1796* (2), 75–90.

(6) Batlle, E., Sancho, E., Franci, C., Dominguez, D., Monfar, M., Baulida, J., and Garcia De Herreros, A. (2000) The transcription factor snail is a repressor of E-cadherin gene expression in epithelial tumour cells. *Nat. Cell Biol. 2* (2), 84–89.

(7) Cano, A., Perez-Moreno, M. A., Rodrigo, I., Locascio, A., Blanco, M. J., del Barrio, M. G., Portillo, F., and Nieto, M. A. (2000) The transcription factor snail controls epithelial-mesenchymal transitions by repressing E-cadherin expression. *Nat. Cell Biol. 2* (2), 76–83.

(8) Comijn, J., Berx, G., Vermassen, P., Verschueren, K., van Grunsven, L., Bruyneel, E., Mareel, M., Huylebroeck, D., and von Roy, F. (2001) The two-handed E box binding zinc finger protein SIP1 downregulates E-cadherin and induces invasion. *Mol. Cell 7* (6), 1267–1278.

(9) Hajra, K. M., Chen, D. Y., and Fearon, E. R. (2002) The SLUG zinc-finger protein represses E-cadherin in breast cancer. *Cancer Res. 62* (6), 1613–1618.

(10) Perez-Moreno, M. A., Locascio, A., Rodrigo, I., Dhondt, G., Portillo, F., Nieto, M. A., and Cano, A. (2001) A new role for E12/E47 in the repression of E-cadherin expression and epithelial-mesenchymal transitions. *J. Biol. Chem. 276* (29), 27424–27431.

(11) Hennig, G., Behrens, J., Truss, M., Frisch, S., Reichmann, E., and Birchmeier, W. (1995) Progression of carcinoma cells is associated with alterations in chromatin structure and factor binding at the E-cadherin promoter in vivo. *Oncogene 11* (3), 475–484.

(12) Yoshiura, K., Kanai, Y., Ochiai, A., Shimoyama, Y., Sugimura, T., and Hirohashi, S. (1995) Silencing of the E-cadherin invasion-suppressor gene by CpG methylation in human carcinomas. *Proc. Natl. Acad. Sci. U.S.A. 92* (16), 7416–7419.

(13) Yoo, C. B., and Jones, P. A. (2006) Epigenetic therapy of cancer: past, present and future. *Nat. Rev. Drug Discovery 5* (1), 37–50.

(14) von Burstin, J., Eser, S., Paul, M. C., Seidler, B., Brandl, M., Messer, M., von Werder, A., Schmidt, A., Mages, J., Pagel, P., Schnieke, A., Schmid, R. M., Schneider, G., and Sauer, D. (2009) E-cadherin regulates metastasis of pancreatic cancer in vivo and is suppressed by a SNAIL/HDAC1/HDAC2 repressor complex. *Gastroenterology 137* (1), 361–371.e5.

(15) Frixen, U. H., Behrens, J., Sachs, M., Eberle, G., Voss, B., Warda, A., Lochner, D., and Birchmeier, W. (1991) E-cadherin-mediated cell-cell adhesion prevents invasiveness of human carcinoma cells. *J. Cell Biol. 113* (1), 173–85.

(16) Onder, T. T., Gupta, P. B., Mani, S. A., Yang, J., Lander, E. S., and Weinberg, R. A. (2008) Loss of E-cadherin promotes metastasis via multiple downstream transcriptional pathways. *Cancer Res. 68* (10), 3645–3654.

(17) Perl, A. K., Wilgenbus, P., Dahl, U., Semb, H., and Christofoti, G. (1998) A causal role for E-cadherin in the transition from adenoma to carcinoma. *Nature 392* (6672), 190–193.

(18) Vleminckx, K., Vakaet, L., Jr., Mareel, M., Fiers, W., and von Roy, F. (1991) Genetic manipulation of E-cadherin expression by epithelial tumor cells reveals an invasion suppressor role. *Cell 66* (1), 107–119.

(19) Birchmeier, W., and Behrens, J. (1994) Cadherin expression in carcinomas: role in the formation of cell junctions and the prevention of invasiveness. *Biochim. Biophys. Acta 1198* (1), 11–26.

(20) Hirohashi, S. (1998) Inactivation of the E-cadherin-mediated cell adhesion system in human cancers. *Am. J. Pathol. 153* (2), 333–9.
(21) van Roy, F., and Berx, G. (2008) The cell-cell adhesion molecule E-cadherin. *Cell. Mol. Life Sci. 65* (23), 3756–3788.
(22) Al-Moundhri, M. S., Al-Khanbashi, M., Al-Kindi, M., Al-Nabhani, M., Burney, I. K., Al-Farsi, A., and Al-Bahrani, B. (2010) Association of E-cadherin (CDH1) gene polymorphisms and gastric cancer. *World J. Gastroenterol. 16* (27), 3432–3436.
(23) Bolos, V., Peinado, H., Perez-Moreno, M. A., Fraga, M. F., Esteller, M., and Cano, A. (2003) The transcription factor Slug represses E-cadherin expression and induces epithelial to mesenchymal transitions: a comparison with Snail and E47 repressors. *J. Cell Sci. 116* (Pt 3), 499–511.
(24) Hewitt, R. E., McMarlin, A., Kleiner, D., Wersto, R., Martin, P., Tsokos, M., Stamp, G. W., and Stetler-Stevenson, W. G. (2000) Validation of a model of colon cancer progression. *J. Pathol. 192* (4), 446–454.
(25) Kramer, O. H., Knauer, S. K., Greiner, G., Jandt, E., Reichardt, S., Guhrs, K. H., Stauber, R. H., Bohmer, F. D., and Heinzel, T. (2009) A phosphorylation-acetylation switch regulates STAT1 signaling. *Genes Dev. 23* (2), 223–235.
(26) Dhawan, P., Singh, A. B., Deane, N. G., No, Y., Shiou, S. R., Schmidt, C., Neff, J., Washington, M. K., and Beauchamp, R. D. (2005) Claudin-1 regulates cellular transformation and metastatic behavior in colon cancer. *J. Clin. Invest. 115* (7), 1765–1776.
(27) Zhang, J. H., Chung, T. D., and Oldenburg, K. R. (1999) A simple statistical parameter for use in evaluation and validation of high throughput screening assays. *J. Biomol. Screening 4* (2), 67–73.
(28) MacCalman, C. D., Brodt, P., Doublet, J. D., Jednak, R., Elhilali, M. M., Bazinet, M., and Blaschuk, O. W. (1994) The loss of E-cadherin mRNA transcripts in rat prostatic tumors is accompanied by increased expression of mRNA transcripts encoding fibronectin and its receptor. *Clin. Exp. Metastasis 12* (2), 101–107.